Journal of Molecular Catalysis A: Chemical 335 (2011) 105–111

Contents lists available at ScienceDirect

Journal of Molecular Catalysis A: Chemical

journal homepage: www.elsevier.com/locate/molcata

Influence of Br^- and Na^+ in synthesis of Silicalite-1 on catalytic performance in vapor phase Beckmann rearrangement of cyclohexanone oxime

Fanhui Meng, Yaquan Wang*, Lina Wang, Rumin Yang, Teng Zhang

Key Laboratory for Green Chemical Technology, School of Chemical Engineering and Technology, Tianjin University, 92# Weijin Road, Nankai District, Tianjin 300072, PR China

ARTICLE INFO

Article history:
Received 20 September 2010
Received in revised form
16 November 2010
Accepted 17 November 2010
Available online 24 November 2010

Keywords:
Silicalite-1
Cyclohexanone oxime
Vapor phase Beckmann rearrangement
ε-Caprolactam
Na^+

ABSTRACT

Silicalite-1 was hydrothermally synthesized with tetrapropylammonium hydroxide (TPAOH) as the template in the presence of various Br^- and Na^+ concentrations, characterized by XRD, SEM, BET, XPS, FT-IR and NH_3-TPD and studied in the vapor phase Beckmann rearrangement of cyclohexanone oxime. The characterization results show that the crystal sizes of Silicalite-1 increase with the increase of Na^+ concentrations in the synthesis; Na^+ is combined in the Silicalite-1 crystals, but removed by a base treatment. The base treated catalysts exhibit nearly complete conversion of cyclohexanone oxime with above 95% selectivity to ε-caprolactam. Catalysts with the addition of up to 20 mol% Br^- relative to TPAOH without Na^+ in the synthesis do not influence the physical and chemical as well as the catalytic properties. The addition of Na^+ below 2.5 mol% of TPAOH do not influence the catalytic properties either. However, at the concentrations of $Na^+ \geq 5$ mol% of TPAOH in the synthesis, the catalysts deactivate faster with the increase of Na^+ contents, which is attributed to more carbon deposition in the larger Silicalite-1 particles, determined by TGA. The results of this work are of great importance for the industry.

1. Introduction

ε-Caprolactam is the monomer for the production of Nylon-6 [1–4]. The current industrial route for the production of ε-caprolactam is a liquid phase Beckmann rearrangement of cyclohexanone oxime using highly concentrated sulfuric acid. Although the process is highly selective, it has several disadvantages such as the corrosion of the reactor, environmental pollutions and by-production of a large amount of ammonium sulfate [1]. In order to solve these problems, strenuous efforts have been devoted to developing vapor phase Beckmann rearrangement of cyclohexanone oxime.

Many solid acid catalysts [5], such as tungsten oxide [6], silica-tantalum oxide [7], sulfated zirconia [8], and boron supported on silica [9], zirconia [10], titania–zirconia [11] are investigated for the vapor phase Beckmann rearrangement reaction. However, these catalysts exhibit low catalytic activities or fast deactivation. Molecular sieves have also been widely investigated for this reaction, such as aluminum- or boron-containing M41S [12–14], SBA-15 [15,16], Mordenite [17,18], FAU-type Y (HUSY) [19–21], BEA-type Beta [17,22–25], and MFI-type ZSM-5 [26–32], TS-1 [26,33] and Silicalite-1 (S-1) [4,26,34–45]. Among these, MFI-type zeolites with high Si/Al atomic ratios and S-1 have been found being active and selective catalysts in the reaction. Sumitomo Chemical Co., Ltd. has commercialized the vapor phase Beckmann rearrangement of cyclohexanone oxime using S-1 as catalyst [4,28,34,35].

In the synthesis of S-1, tetrapropylammonium hydroxide (TPAOH) is used as the template and alkali source. However, Br^- and Na^+ are often found as impurities in TPAOH, which is produced through an ionic exchange process. Intentional addition of sodium to ZSM-5 or TiO_2 led to the increase of the crystal sizes and affected the morphology [46–48]. However, the effects of Br^- and Na^+ in the synthesis of S-1 on the crystal sizes, morphology and the catalytic performance in the vapor phase Beckmann rearrangement of cyclohexanone oxime has not been studies.

In this work, Br^- and Na^+ are added into the TPAOH solution for the synthesis of S-1. The obtained S-1 catalysts are characterized with XRD, SEM, BET, XPS, FT-IR and NH_3-TPD and investigated in the vapor phase Beckmann rearrangement of cyclohexanone oxime. The aims are to study the effects of Br^- and Na^+ in the synthesis on S-1 crystal structure, morphology and the catalytic performance.

2. Experimental

2.1. Materials

Electronic grade tetraethyl orthosilicate (TEOS) was obtained from Tianjin Kermel Chemical Reagents. Sodium hydroxide (NaOH) and methanol were purchased from Tianjin Guangfu Fine Chemical Research Institute. TPAOH aqueous solution (10 wt%, $Na^+ < 4$ ppm

* Corresponding author. Tel.: +86 22 23507881; fax: +86 22 23507881.
E-mail address: yqwang@tju.edu.cn (Y. Wang).

1381-1169/$ – see front matter © 2010 Elsevier B.V. All rights reserved.
doi:10.1016/j.molcata.2010.11.021

and no bromine was found by Ag^+ testing) was prepared through the ionic exchange of tetrapropylammonium bromide (TPABr), which was purchased from Tianjin Guangfu Fine Chemical Research Institute.

2.2. Catalyst preparation

The starting materials for the hydrothermal synthesis of S-1 had the following molar compositions: 435 SiO_2:100TPAOH:*x*TPABr:*x*NaOH:20870 H_2O. First, the required amounts of TPABr and NaOH were dissolved in TPAOH aqueous solution in a polypropylene bottle under stirring, then TEOS was added in TPAOH aqueous solution. The resulting mixture was stirred vigorously at room temperature for 2 h, and the crystallization was performed in a PTFE-lined, stainless steel autoclave under static conditions at 378 K for 96 h. The white solid product was centrifuged and washed with distilled water until the pH reached about 7, then it was dried at 383 K overnight and calcined at 823 K in air for 6 h. The samples are designated as S-1-*x*, with *x* varied at 0, 2.5, 5, 10 and 20, respectively. To investigate the effect of Br^- alone, an S-1 sample was synthesized with *x* of Br^- equal to 20 without the addition of Na^+ with the same procedure. This sample is designated as S-1-20Br.

The samples were treated with a nitrogen-containing basic solution. For this, 4 g samples were treated with a mixture of aqueous ammonium nitrate solution (7.5 wt%, 30 g) and aqueous ammonia solution (25 wt%, 10 g) at 363 K for 1 h for three times. After the treatment, the samples were washed until the pH reached about 7, and then dried at 383 K and calcined at 823 K for 6 h in air.

2.3. Catalyst characterization

X-ray diffraction (XRD) patterns of the samples were taken on a Rigaku D/max 2500 powder diffractometer using graphite monochromator with Cu Kα radiation (λ = 1.5406 Å) at 40 kV and 200 mA with a scanning rate of 8° min^{-1} in the 2θ ranges from 5° to 35°.

Nanosem 430 field emission scanning electron microscopy (FESEM) was utilized to characterize the size and morphology of the samples after sputtering with gold.

BET specific surface areas were measured by N_2 adsorption at 77 K on Micromeritics Tristar 3000. BET specific surface areas were calculated by applying the Brunauer–Emmett–Teller (BET) method.

XPS spectra of the samples before and after the base treatment were measured with a Perkin-Elemer PHI-1600 X-ray photoelectron spectrometer using Mg Kα radiation (1253.6 eV) at 15 kV and 250 W. The binding energies were calibrated by C1s as the reference energy (C1s = 284.6 eV).

FT-IR spectra of the samples before and after the base treatment were recorded on a Nicolet Magna 560 spectrometer with a resolution of 4 cm^{-1}. For this, a self-supported wafer (15 mg/cm^2) was placed in a cell with CaF_2 windows, and heated at 673 K for 1 h under vacuum of 0.1 Pa. When the cell was cooled down to 423 K, the spectra were recorded.

NH_3-TPD spectra were recorded using Micromeritics 2910 chemical adsorption instrument. The samples were pretreated in a nitrogen flow at 823 K for 1 h, and then cooled down to ambient temperature, and ammonia was introduced with nitrogen as the carrier gas. After 30 min, the flow was switched to nitrogen, and the sample was heated to 873 K at a rate of 10 K/min. The desorbed ammonia was monitored by a thermal conductivity detector.

The amounts of coke formed after the Beckmann rearrangement reaction were measured using Shimadzu TGA-50 thermogravimetric analyzer by heating from room temperature to 1123 K at 10 K/min in the flow of air. The weight loss between 623 K and 973 K was attributed to the burning of coke [44].

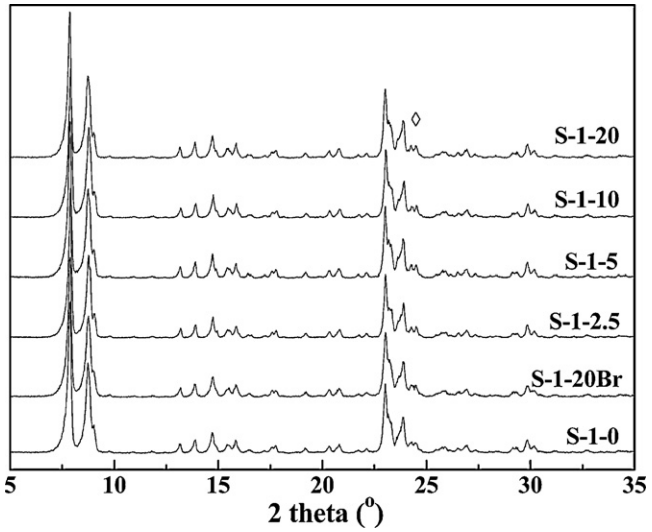

Fig. 1. XRD patterns of base treated samples S-1-*x* synthesized in the presence of various Br^- and Na^+ concentrations.

2.4. Vapor phase Beckmann rearrangement reaction

The catalytic vapor phase Beckmann rearrangement reaction was carried out at atmospheric pressure in a fixed-bed flow reactor. 0.3 g catalyst (shaped under pressure and sieved at 40–60 mesh) was mixed with 2 g quartz sand (40–60 mesh) and positioned with quartz wool in a quartz reactor with an inner diameter of 10 mm and a length of 400 mm. The reactor was placed inside a temperature-controllable vertical furnace. The thermocouple tip in the quartz well was centered at the middle of the catalyst. After treated in a flow of Ar at 673 K for 1 h, a mixture with 30 wt% cyclohexanone oxime and 1 wt% water in methanol was fed into the reactor at the oxime weight hourly space velocity (WHSV) of 6 h^{-1} by a double-plunger micro-metering pump at the rate of 6 cm^3/h, and 30 cm^3/min of Ar (99.99%) was introduced using a mass flow controller. These optimized conditions were obtained in the previous works [23,25,44]. The reaction products were collected in an ice-water trap and analyzed with an HP 4890GC equipped with an OV-1701 column and a flame ionization detector.

3. Results and discussion

3.1. Characterization results

The powder XRD patterns of the base treated S-1 samples synthesized in the presence of different Br^- and Na^+ concentrations are given in Fig. 1. It is seen that all the samples are highly crystalline, the XRD patterns show all reflections matching well with those reported for S-1 [49], and no peaks corresponding to Na-containing phases are detected. All samples show reflections at 2θ = 24.4°, indicating that the typical structures of the S-1 are monoclinic symmetry [36,40]. The relative crystallinity of the base treated S-1 are calculated by comparing the total intensity values of the reflections at 2θ = 7.9°, 8.9°, 23.0°, 23.2°, 23.7° and 24.0° [50] and assuming those of S-1-0 being 100%. The results in Table 1 indicate that S-1 with various Br^- and Na^+ concentrations in the synthesis have almost the same crystallinity, suggesting that the presence of Br^- alone or with Na^+ together in the synthesis does not affect the crystal structure of S-1.

Fig. 2 shows the SEM micrographs of the base treated samples of S-1-*x* synthesized in the presence of different concentrations of Br^- and Na^+. The micrographs demonstrate a uniform distribution of the crystal sizes for each sample. With the increase of Br^- and

Table 1
Properties of base treated S-1-*x*.

Samples	Relative crystallinity (%)	Crystal size[a] (nm)	S_{BET} (m^2/g)	XPS results		
				Surface Na/Si molar ratios before base treatment[b]	Surface Na/Si molar ratios after base treatment[b]	Theoretical bulk Na/Si molar ratios[c]
S-1-0	100	170	357	0	0	0
S-1-20Br	98	170	345	0	0	0
S-1-2.5	101	180	352	0.006	0	0.0057
S-1-5	104	270	379	0.010	0	0.012
S-1-10	101	280	367	0.021	0	0.023
S-1-20	102	290	363	0.043	0	0.046

[a] Results from SEM micrographs.
[b] Cauculated from Na1s and Si2p peak areas of XPS.
[c] Cauculated from the amounts of NaOH and TEOS added in the synthesis.

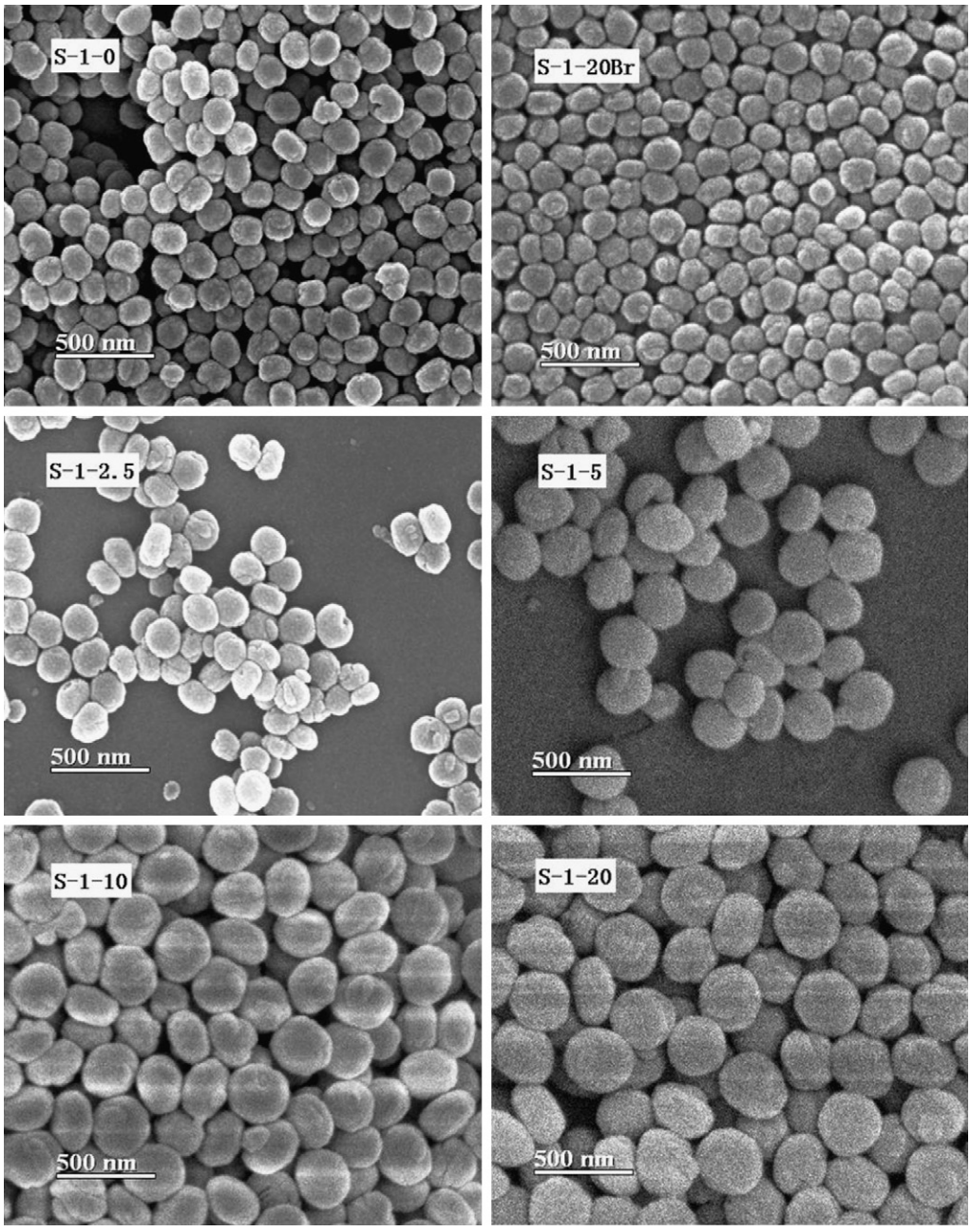

Fig. 2. SEM images of base treated samples S-1-*x* synthesized in the presence of various Br^- and Na^+ concentrations.

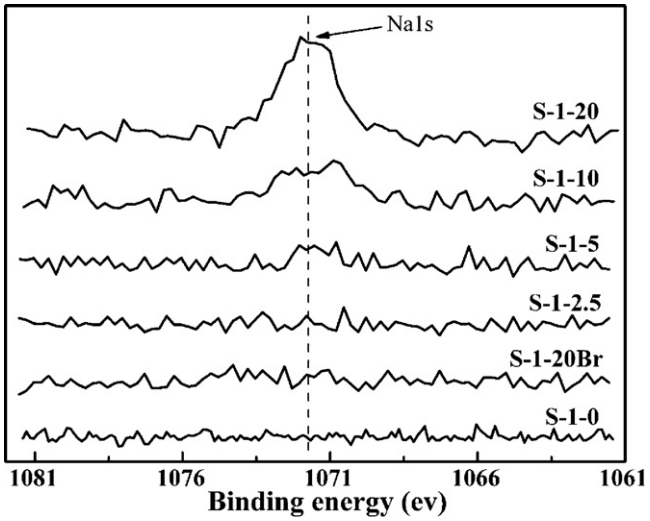

Fig. 3. XPS Na1s spectra of samples S-1-*x* as-synthesized in the presence of various Br^- and Na^+ concentrations.

Na^+ concentrations in the synthesis, the crystal sizes increase, e.g., from 170 nm in the absence of Br^- and Na^+ to 180 nm at $x = 2.5$ of Br^- and Na^+ in the synthesis, then sharply to 270 nm and 290 nm at $x = 5$ and 20, respectively, as shown in Table 1. The presence of 20 mol% TPABr alone without the addition of Na^+ in the synthesis (S-1-20Br) does not affect the crystal size and the morphology of S-1. Our previous studies [51] showed that the crystal sizes of S-1 were the same when TPAOH/SiO_2 molar ratios increased from 0.2 to 0.3. In the present work, the highest TPAOH/SiO_2 molar ratio is 0.276. So, the increase of the crystal sizes of S-1 would not be caused by the increase of OH^- due to the addition of NaOH. Instead, it can be concluded that the increase of the crystal sizes of S-1 mainly results from the presence of Na^+ in the synthesis. Choudhary and Akolekar [52] found that the addition of NaCl, KCl and ammonia in the synthesis mixture, using fumed silica as silica source, also resulted in S-1 with larger crystal sizes. It was reported that in the syntheses of ZSM-5 and TiO_2, the crystal sizes also increased with the increase of Na^+ contents in the synthesis [46–48]. Persson et al. [46] monitored the crystal growth of ZSM-5 using the direct method of dynamic light scattering and found that the introduction of sodium to the synthesis mixture increased the crystal growth rate as compared with that in the sodium-free mixture, but decreased the number of the crystals formed, and therefore the crystal sizes increased. This might be also the reason why the presence of Na^+ increases the crystal sizes of S-1. Of course, it is worthy to be studied further.

The BET specific surface areas of the base treated S-1-*x* catalysts are listed in Table 1. It is seen that the BET specific surface areas of all the catalysts are around 360 m^2/g, implying that the introducing of Br^- and Na^+ to the synthesis mixture have neglected effect on the BET specific surface areas.

Na1s spectra of XPS before the base treatment of S-1-*x* samples synthesized in the presence of different Br^- and Na^+ concentrations in the syntheses are shown in Fig. 3. No spectra of Na1s were detected in the absence of Na^+ (S-1-0 and S-1-20Br) or at very low concentration of Na^+ (S-1-2.5) in the S-1 synthesis. With the increase of Na^+ equal to or above 5 mol% relative to TPAOH in the synthesis, the Na1s spectra appear and become stronger and stronger. The XPS results in Table 1 show that the molar ratios of Na/Si on the S-1 surface increase with the increase of Na^+ concentrations in the synthesis and agree well with the theoretical bulk values of Na/Si. The results indicate that Na^+ is stoichiometrically combined in the S-1 crystals and there is no surface enrichment of Na^+. After the base treatment, there is no spectra of Na1s being detected (the corresponding XPS spectra are just lines with noises and are not given), implying that Na^+ in the S-1 has been removed by the treatment with nitrogen-containing basic solution.

FT-IR spectra of S-1-*x* samples before and after the base treatment in the range of 3800–3200 cm^{-1} are compared in Fig. 4. It has been reported that the peak around 3740 cm^{-1} is due to the terminal silanols on the catalyst surfaces, and the bands around 3690 cm^{-1} and 3500 cm^{-1} represent the vicinal silanols and silanol nests, respectively [3,36]. As shown in Fig. 4, before the base treatment with the nitrogen-containing solution, all samples show a sharp peak around 3740 cm^{-1} from the terminal silanols. After the base treatment, the 3740 cm^{-1} peak of the terminal silanols disappear, and two broad bands around 3690 cm^{-1} and 3500 cm^{-1}, corresponding to the vicinal silanols and silanol nests, respectively, become apparent. It has also been reported that the vicinal silanols and silanol nests are favorable for the formation of ε-caprolactam, while the terminal silanols are responsible for the formation of the by-products [3,22,27,36]. Therefore, it is expected that the catalytic performance of the catalysts can be improved by the base treatment.

The surface acidity of the samples before and after the base treatment was characterized by NH_3-TPD, but no peaks were detected over all the samples at the temperature above 423 K under the conditions used in our previous works [44], implying that the samples do not exhibit strong acid sites. The results are in accordance with those of Matsumura [53].

3.2. Catalytic performance in the Beckmann rearrangement

The S-1-*x* catalysts are investigated for the vapor phase Beckmann rearrangement of cyclohexanone oxime reaction. Without the base treatment, the catalysts give above 99% initial conversion of cyclohexanone oxime, but only around 90% selectivity to ε-caprolactam, which is much lower than at least 95% selectivity required by industry. Instead, all the catalysts after the base treatment exhibit both very high conversions of cyclohexanone oxime (Fig. 5a) and very high selectivity to ε-caprolactam (Fig. 5b). Therefore, only the catalysts after the base treatment are studied in detail.

As mentioned above, the vicinal silanols and silanol nests are favorable species for the formation of ε-caprolactam in the vapor phase Beckmann rearrangement, while the terminal silanols are favorable for the formation of by-products [3,22,27,36]. After the base treatment, the terminal silanols are removed and the vicinal silanols and silanol nests on all the catalysts appear in large quantity. This may be the reason why all the catalysts give nearly complete conversion of cyclohexanone oxime and high selectivity to ε-caprolactam.

In order to find out if there are differences between the catalysts in terms of the stability, the reaction was conducted at high oxime WHSV of 6 h^{-1}. In fact, WHSV of 1–2 h^{-1} is high enough for the industry. The other parameters influencing the reaction have been optimized in our previous studies [23,25,44]. The results in Fig. 5 show that all the catalysts exhibit a very high initial conversion of cyclohexanone oxime, above 99.9% (Fig. 5a). As to the selectivity (Fig. 5b), no appreciable differences are found among all the catalysts within the testing time. In the absence of Na^+ in the synthesis, the catalyst S-1-0 shows very good stability: after 36.5 h on stream, the conversion of cyclohexanone oxime is still above 99.4%. This catalyst is accepted by an industrial company. With the addition of Br^- and Na^+ at $x = 2.5$ in the synthesis, the catalyst S-1-2.5 shows the same stability as S-1-0. However, with the further increase of $x = 5$ or above in the synthesis, the catalysts deactivate faster, e.g., after 30.5 h on stream, S-1-5, S-1-10 and S-1-20 exhibit the conversions of 99.4%, 98.6% and 98.2%, respectively, while that of S-1-0 is 99.6%.

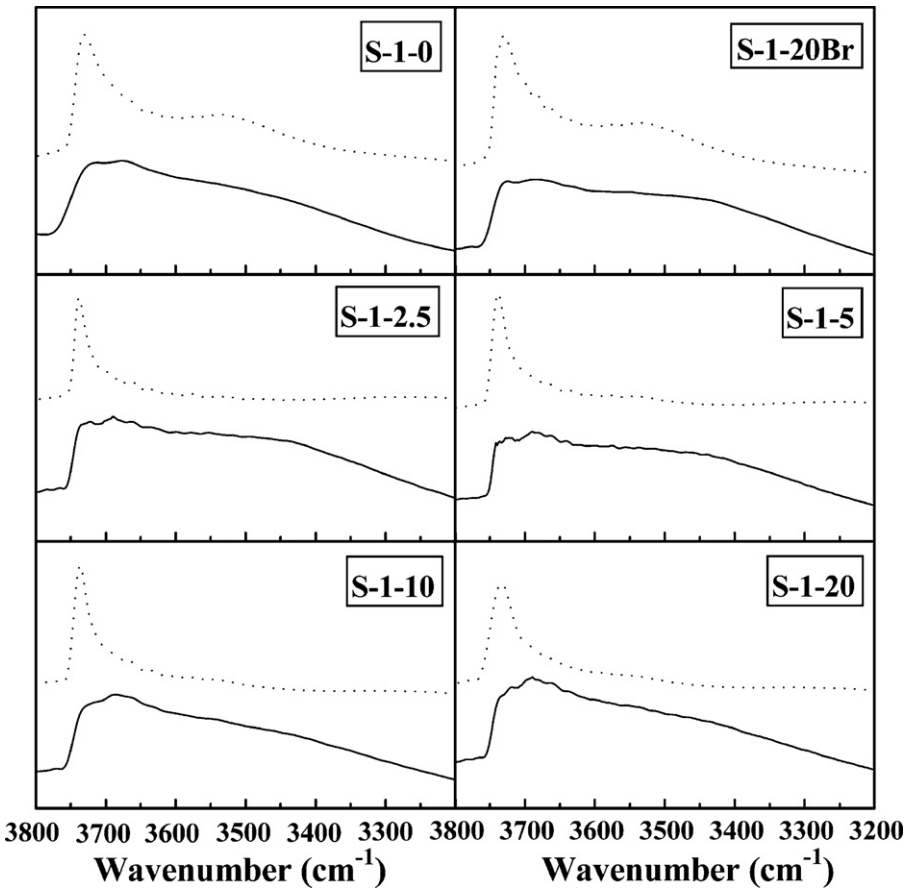

Fig. 4. FT-IR spectra of S-1 samples synthesized in the presence of various Br^- and Na^+ concentrations before and after base treatment. Dot lines represent the samples before base treatment, and solid lines represent samples after base treatment.

It is seen that the catalyst S-1-20Br, prepared with the addition of Br^- at $x = 20$ without the addition of Na^+ in the synthesis, show the same stability as S-1-0. So, it can be concluded that the differences in the stability are not resulted from the addition of Br^- in the synthesis.

In studying the catalytic properties of HNaY zeolite in the vapor phase Beckmann rearrangement, it was found that the acid centers and Na^+ in the HNaY zeolite are responsible for the formation of by-products, especially 5-cyanopent-1-ene [19,54]. Matsumura et al. [53,55] reported that the Na^+-modified S-1 does not exhibit strong acid sites, and concluded that the sodium ions in S-1 play an important role for the dehydrogenation of methanol. It was also found that strong acid centers could cause catalyst deactivation in the vapor phase Beckmann rearrangement [18,19,30,54]. In the present work, the XPS results show that Na^+ is combined in the S-1 crystals; however, after the base treatment, all the Na^+ species are depleted. One may argue that the removal of Na^+ from the S-1 surface may result in the formation of H^+, the acid centers. However, the FT-IR results clearly show that the terminal silanols, the strongest acid centers on S-1, are removed after the base treatment. In addition, NH_3-TPD results show that either before or after the base treatment, no catalyst exhibit any strong acid centers. As mentioned above, the properties of S-1 were not affected when the TPAOH/SiO_2 molar ratios increased from 0.2 to 0.3 [51]. So, the faster deactivation of the catalysts synthesized in the presence of Na^+ cannot be attributed to the OH^- anions in the synthesis or the sodium cations combined in the catalysts.

The only differences of the catalysts found by the characterizations are the crystal sizes. SEM results show that the crystal size of S-1-20Br with the addition of up to 20 mol% Br^- relative to TPAOH in the absence of Na^+ in the synthesis is exactly the same as that of S-1-0. That is maybe why the stability of S-1-20Br is the same as that of S-1-0. When the concentration of Na^+ is at $x = 2.5$ in the synthesis, the crystal size of S-1-2.5 is not appreciably larger than that of S-1-0. Therefore, the stability S-1-2.5 is also the same as that of S-1-0.

Kath et al. [38] reported that both cyclohexanone oxime and ε-caprolactam have access to the micropores of S-1, and the Beckmann rearrangement can take place in the micropores. Nevertheless, since S-1 is a microporous zeolite with three-dimensional network of 10-membered ring channels, and the molecules of the product ε-caprolactam are larger than cyclohexanone oxime, the difficult diffusion may cause carbon deposition. With the further increase of Br^- and Na^+ concentration at $x \geq 5$, the S-1 crystals sizes increase sharply, e.g., to 270 nm or above. It is conceivable that the diffusion of the product would be much more difficult from the larger S-1 crystals compared with the smaller ones because the smaller crystals get the shorter diffusion pathways. Not to mention the other larger by-product molecules produced in the reaction. So, those catalysts with the larger crystal sizes deactivate much faster.

After the Beckmann rearrangement reaction, the catalysts were subjected to TGA measurements in the presence of air. The results in Fig. 6 show that with the increase of the crystal sizes of S-1-*x*, the amounts of coke increase after the reaction. These results agree with the hypothesis that the larger S-1 crystals may cause the diffusion of the products and by-products more difficult and result in more coke formation, and therefore the catalysts deactivate faster.

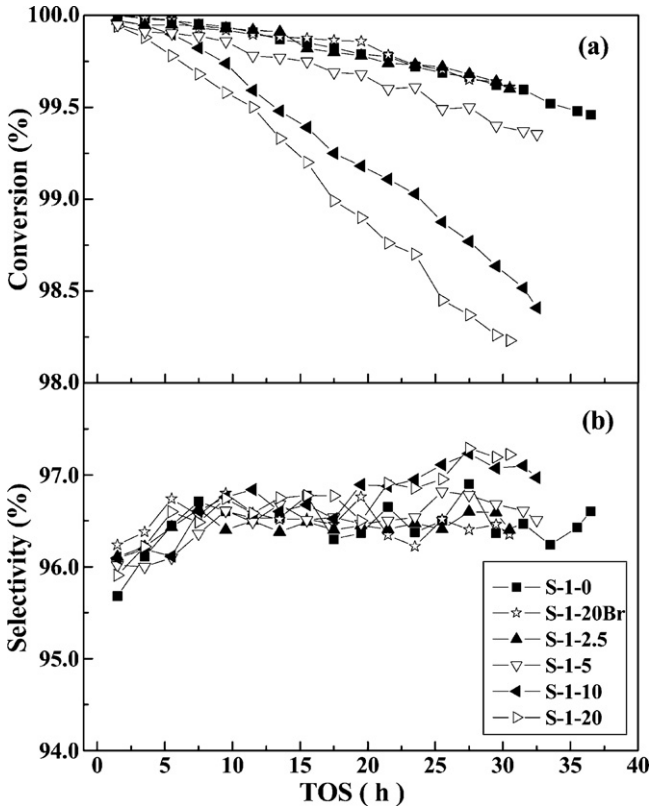

Fig. 5. Changes of conversion of cyclohexanone oxime and selectivity to ε-caprolactam with time on stream. Reaction conditions: 638 K, 0.1 MPa, WHSV = 6 h^{-1}, 30 wt% cyclohexanone oxime and 1 wt% water in methanol.

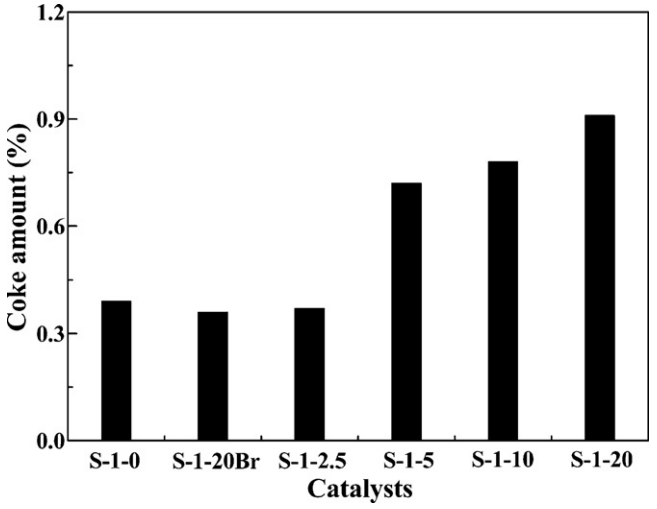

Fig. 6. Amounts of coke formed after the reaction over base treated S-1 catalysts.

4. Conclusions

S-1 has been synthesized in the presence of various Br^- and Na^+ concentrations. After the base treatment with a nitrogen-containing solution, all the catalysts exhibit nearly complete conversion with very high selectivity in the vapor phase Beckmann rearrangement of cyclohexanone oxime. The addition of up to 20 mol% Br^- alone or Na^+ concentration below 2.5 mol% relative to TPAOH in the synthesis does not change the properties of S-1. But when the concentration of Na^+ is equal to or above 5 mol% relative to TPAOH in the synthesis, with the increase of Na^+ concentration in the synthesis, the crystal sizes of S-1 increase, and the catalysts deactivate faster in the reaction. The stabilities of the catalysts can be correlated with the crystal sizes of S-1, i.e., the larger the crystal sizes of S-1, the faster the catalysts deactivate.

Acknowledgement

The authors gratefully acknowledge the financial support by Tianchen Corp. China.

References

[1] G. Dahlhoff, J.P.M. Niederer, W.F. Hölderich, Catal. Rev. 43 (2001) 381–441.
[2] A. Corma, H. Garcia, Chem. Rev. 103 (2003) 4307–4366.
[3] W.F. Hölderich, J. Röseler, G. Heitmann, A.T. Liebens, Catal. Today 37 (1997) 353–366.
[4] Y. Izumi, H. Ichihashi, Y. Shimazu, M. Kitamura, H. Sato, Bull. Chem. Soc. Jpn. 80 (2007) 1280–1287.
[5] N.R. Candeias, C.A.M. Afonso, J. Mol. Catal. A: Chem. 242 (2005) 195–217.
[6] N. Kob, R.S. Drago, Catal. Lett. 49 (1997) 229–234.
[7] T. Ushikubo, K. Wada, J. Catal. 148 (1994) 138–148.
[8] B.M. Reddy, G.K. Reddy, K.N. Rao, L. Katta, J. Mol. Catal. A: Chem. 306 (2009) 62–68.
[9] S. Sato, K. Urabe, Y. Izumi, J. Catal. 102 (1986) 99–108.
[10] B.Q. Xu, S.B. Cheng, S. Jiang, Q.M. Zhu, Appl. Catal. A: Gen. 188 (1999) 361–368.
[11] D.S. Mao, G.Z. Lu, Q.L. Chen, J. Mol. Catal. A: Chem. 240 (2005) 164–171.
[12] K. Chaudhari, R. Bal, A.J. Chandwadkar, S. Sivasanker, J. Mol. Catal. A: Chem. 177 (2002) 247–253.
[13] L. Forni, C. Tosi, G. Fornasari, F. Trifir, A. Vaccari, J.B. Nagy, J. Mol. Catal. A: Chem. 221 (2004) 97–103.
[14] T.D. Conesa, R. Luque, J.M. Campelo, D. Luna, J.M. Marinas, A.A. Romero, J. Mater. Sci. 44 (2009) 6741–6746.
[15] A. Bordoloi, S.B. Halligudi, Appl. Catal. A: Gen. 379 (2010) 141–147.
[16] V.R. Reddy Marthala, J. Frey, M. Hunger, Catal. Lett. 135 (2010) 91–97.
[17] P. O'Sullivan, L. Forni, B.K. Hodnett, Ind. Eng. Chem. Res. 40 (2001) 1471–1475.
[18] T. Takahashi, M.N.A. Nasution, T. Kai, Appl. Catal. A: Gen. 210 (2001) 339–344.
[19] A. Aucejo, M.C. Burguet, A. Corma, V. Fornes, Appl. Catal. 22 (1986) 187–200.
[20] L.X. Dai, K. Koyama, M. Miyamoto, T. Tatsumi, Appl. Catal. A: Gen. 189 (1999) 237–242.
[21] J. Sirijaraensre, J. Limtrakul, ChemPhysChem 7 (2006) 2424–2432.
[22] G.P. Heitmann, G. Dahlhoff, W.F. Hölderich, Appl. Catal. A: Gen. 185 (1999) 99–108.
[23] Y.J. Zhang, Y.Q. Wang, Y.F. Bu, Z.T. Mi, W. Wu, E.Z. Min, S. Han, S.B. Fu, Catal. Commun. 6 (2005) 53–56.
[24] A.B. Fernández, A. Marinas, T. Blasco, V. Fornés, A. Corma, J. Catal. 243 (2006) 270–277.
[25] Y.J. Zhang, Y.Q. Wang, Y.F. Bu, Microporous Mesoporous Mater. 107 (2008) 247–251.
[26] A. Thangaraj, S. Sivasanker, P. Ratnasamy, J. Catal. 137 (1992) 252–256.
[27] G.P. Heitmann, G. Dahlhoff, J.P.M. Niederer, W.F. Hölderich, J. Catal. 194 (2000) 122–129.
[28] H. Ichihashi, M. Kitamura, Catal. Today 73 (2002) 23–28.
[29] H. Ichihashi, M. Ishida, A. Shiga, M. Kitamura, T. Suzuki, K. Suenobu, K. Sugita, Catal. Surv. Asia 7 (2003) 261–270.
[30] T. Takahashi, T. Kai, E. Nakao, Appl. Catal. A: Gen. 262 (2004) 137–142.
[31] J. Sirijaraensre, J. Limtrakul, Phys. Chem. Chem. Phys. 11 (2009) 578–585.
[32] I. Lezcano-Gonzalez, M. Boronat, T. Blasco, Solid State Nucl. Magn. Reson. 35 (2009) 120–129.
[33] R. Palkovits, W. Schmidt, Y. Ilhan, A. Erdem-Senatalar, F. Schüth, Microporous Mesoporous Mater. 117 (2009) 228–232.
[34] M. Kitamura, H. Ichihashi, H. Tojima, US Patent 5,212,302 (1993).
[35] H. Ichihashi, K. Sugita, M. Yako, US Patent 6,303,099 (2001).
[36] G.P. Heitmann, G. Dahlhoff, W.F. Hölderich, J. Catal. 186 (1999) 12–19.
[37] T. Komatsu, T. Maeda, T. Yashima, Microporous Mesoporous Mater. 35–36 (2000) 173–180.
[38] H. Kath, R. Gläser, J. Weitkamp, Chem. Eng. Technol. 24 (2001) 150–153.
[39] C. Flego, L. Dalloro, Microporous Mesoporous Mater. 60 (2003) 263–271.
[40] L. Forni, G. Fornasari, G. Giordano, C. Lucarelli, A. Katovic, F. Trifirò, C. Perri, J.B. Nagy, Phys. Chem. Chem. Phys. 6 (2004) 1842–1847.
[41] W.C. Li, A.H. Lu, R. Palkovits, W. Schmidt, B. Spliethoff, F. Schüth, J. Am. Chem. Soc. 127 (2005) 12595–12600.
[42] V.R. Reddy Marthala, Y. Jiang, J. Huang, W. Wang, R. Glaser, M. Hunger, J. Am. Chem. Soc. 128 (2006) 14812–14813.
[43] B. Bonelli, L. Forni, A. Aloise, J.B. Nagy, G. Fornasari, E. Garrone, A. Gedeon, G. Giordano, F. Trifirò, Microporous Mesoporous Mater. 101 (2007) 153–160.
[44] Y.F. Bu, Y.Q. Wang, Y.J. Zhang, L. Wang, Z.T. Mi, W. Wu, E.Z. Min, S.B. Fu, Catal. Commun. 8 (2007) 16–20.
[45] A. Cesana, S. Palmery, R. Buzzoni, G. Spanò, F. Rivetti, L. Carnelli, Catal. Today 154 (2010) 264–270.
[46] A.E. Persson, B.J. Schoeman, J. Sterte, J.E. Otterstedt, Zeolites 15 (1995) 611–619.
[47] R. Van Grieken, J.L. Sotelo, J.M. Menéndez, J.A. Melero, Microporous Mesoporous Mater. 39 (2000) 135–147.

[48] H.J. Nam, T. Amemiya, M. Murabayashi, K. Itoh, Res. Chem. Intermed. 31 (2005) 365–370.
[49] E.M. Flanigen, J.M. Bennett, R.W. Grose, J.P. Cohen, R.L. Patton, R.M. Kirchner, J.V. Smith, Nature 271 (1978) 512–516.
[50] F. Feng, K.J. Balkus, Microporous Mesoporous Mater. 69 (2004) 85–96.
[51] Y.F. Bu, MFI zeolites for the vapor phase Beckmann rearrangement of cyclohexanone oxime, Ph.D. Degree, Tianjin University, Tianjin, 2005.
[52] V.R. Choudhary, D.B. Akolekar, Mater. Chem. Phys. 20 (1988) 299–308.
[53] Y. Matsumura, K. Hashimoto, S. Yoshida, J. Chem. Soc., Faraday Trans. 1 84 (1988) 87–96.
[54] J.D. Butler, T.C. Poles, J. Chem. Soc., Perkin Trans. 2 (1973) 1262–1266.
[55] Y. Matsumura, K. Hashimoto, H. Kobayashi, S. Yoshida, J. Chem. Soc., Faraday Trans. 86 (1990) 561–565.